Proceedings of the Seventeenth International Conference on
Civil, Structural and Environmental Engineering Computing
Edited by: P. Iványi, J. Kruis and B.H.V. Topping
Civil-Comp Conferences, Volume 6, Paper 2.8
Civil-Comp Press, Edinburgh, United Kingdom, 2023
doi: 10.4203/ccc.6.2.8

Identification of Bridge Mode Shapes from a Two-Axle Test Vehicle by Wavelet Transform

H. Xu,[1] X.Y. Chen,[2] Z.L. Wang,[1] K. Shi,[1] and Y.B. Yang[1]

[1]School of Civil Engineering, Chongqing University
Chongqing, P.R. China
[2]College of Civil Engineering, Hunan University
Changsha, P.R. China

Abstract

Wavelet transform (WT) is theoretically investigated to recover bridge mode shapes from a passing two-axle test vehicle by using the correlation between the front and rear contact points. In this study, closed-form solutions for the dynamic responses of the bridge and front and rear contact points are derived. To overcome the masking effect by vehicle's self frequencies on bridge frequencies in the vehicle's spectra, the procedure for calculating contact responses of a two-axle test vehicle considering the suspension effect was derived. Next, the procedure for constructing bridge mode shapes using the WT is proposed and theoretically investigated. The efficacy of the proposed procedure is validated by numerical studies.

Keywords: bridge, vehicle, mode shape, wavelet transform, contact, vehicle scanning method

1 Introduction

As critical components of civil infrastructure, bridges play an important role in connecting roads that are separated by natural or artificial barriers. As they are critical to ground transportation and economic development of a region or country, the safety and durability of bridges are always of concern. Previously, to monitor the health status of bridges, vibration-based structure health monitoring (SHM) methods have been widely used, which can provide reference in a timely manner to the bridge

administrators for duty-scheduling and decision-making. For the last half century, the measurement of the bridge response has been primarily based on the direct method, i.e., by installing vibration sensors on the bridge to directly measure the bridge response. For the huge number of bridges existing all over the world, there is an urgent need to develop economical and efficient method that can be widely used in the health monitoring of most bridges.

As part of the effort to tackle the above problem, a moving test vehicle fitted with sensors for extracting the bridge frequencies was proposed by Yang et al. in 2004 [1]. To better interpretation of the meaning implied, such a method was renamed as the *vehicle scanning method* (VSM) for bridges. Primarily, the dynamic response acquired by a moving test vehicle was utilized to extract bridge frequencies by analytical, numerical or experimental studies [1-3]. Subsequently, such a technique has been extended to the identification of other bridge properties, such as mode shapes, damping ratios, and damages. Since the concept of the VSM first proposal in 2004, it has drawn increasing interest from researchers worldwide. Progress on various aspects of the VSM has been achieved in the past nearly two decades [4].

Previously, bridge mode shapes and their derivatives have been widely used for bridge damage identification. To construct bridge mode shapes effectively, techniques such as Hilbert transform [5], short time frequency domain decomposition [6], short-time Fourier transformation [7], matrix completion [8], and wavelet transform (WT) [9] were adopted.

However, as far as the vehicle response is concerned, an annoying fact is that the vehicle's frequencies may appear as striking peaks in the vehicle's spectrum, which may obscure the identification of bridge frequencies. To alleviate such a problem, a simple and efficient way is to use the vehicle-bridge contact response, which can enhance the identification of bridge frequencies. In this study, the procedure for calculating the front and rear contact responses of a two-axle test vehicle considering the suspension effect will be derived.

To construct bridge mode shapes, the time-frequency analysis techniques are particularly attractive, among which the WT is an advanced representative. Through the WT, the time domain response can be transformed to the time-frequency domain, and thus provides information about both time and frequency. In this study, the WT is theoretically investigated to construct bridge mode shapes via the skillful use of the correlation between the front and rear contact points of the two-axle test vehicle.

2 Closed-Form Solutions for Bridge and Contact Responses

With reference to Figure 1, the analysis model adopted is a simply supported beam subjected to a two-axle vehicle moving at speed v. The two-axle test vehicle is modeled as a *four degree-of-freedom* (DOF) system, consisting of car body (two DOFs) and two wheels (one DOF for each wheel). The vehicle's body used is simplified as a rigid beam of mass M_v, mass moment of inertia J_v and length d. The front and rear wheels of masses (m_{wf}, m_{wr}) are connected to the car body through suspension spring-dashpot units of stiffnesses (k_{sf}, k_{sr}) and damping coefficients (c_{vf}, c_{vr}), and in contact with the bridge by wheel spring-dashpot units of stiffnesses

(k_{wf}, k_{wr}) and damping coefficients (c_{wf}, c_{wr}). The distance from the jth axle to the vehicle's center of gravity is denoted by d_j ($j = f, r$).

The equations for the vertical and rotational motions of the car body are

$$\begin{aligned} &M_v\ddot{y}_v + c_{sf}\left[\dot{y}_v - d_f\dot{\theta}_v - \dot{y}_{wf}\right] + c_{sr}\left[\dot{y}_v + d_r\dot{\theta}_v - \dot{y}_{wr}\right] \\ &+k_{sf}\left[y_v - d_f\theta_v - y_{wf}\right] + k_{sr}\left[y_v + d_r\theta_v - y_{wr}\right] = 0, \end{aligned} \tag{1}$$

$$\begin{aligned} &J_v\ddot{\theta}_v - c_{sf}d_f\left[\dot{y}_v - d_f\dot{\theta}_v - \dot{y}_{wf}\right] + c_{sr}d_r\left[\dot{y}_v + d_r\dot{\theta}_v - \dot{y}_{wr}\right] \\ &-k_{sf}d_f\left[y_v - d_f\theta_v - y_{wf}\right] + k_{sr}d_r\left[y_v + d_r\theta_v - y_{wr}\right] = 0. \end{aligned} \tag{2}$$

where y_v and θ_v denote the vertical displacement and rotation, respectively, of the mass center of the vehicle's body, y_{wj} the vertical displacement of the front or rear wheel, and the dot ($\dot{}$) denotes the time derivative.

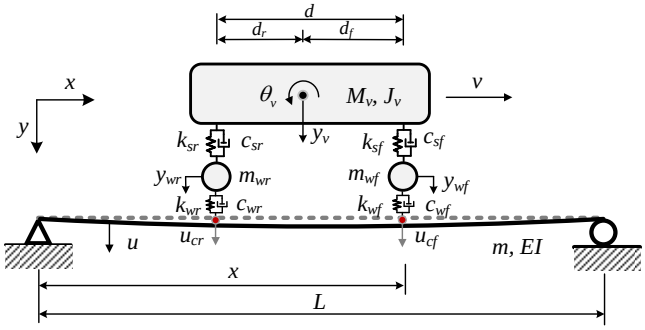

Figure 1 A two-axle vehicle travelling over a simply supported beam [10].

The vertical equation of motion of the front and rear wheels is

$$\begin{aligned} &m_{wj}\ddot{y}_{wj}(t) + c_{wj}\left[\dot{y}_{wj}(t) - \dot{u}_{cj}(t)\right] + k_{wj}\left[y_{wj}(t) - u_{cj}(t)\right] \\ &= c_{sj}\left[\dot{y}_{vj}(t) - \dot{y}_{wj}(t)\right] + k_{sj}\left[y_{vj}(t) - y_{wj}(t)\right], \qquad j = f, r. \end{aligned} \tag{3}$$

Here, $u(x,t)$ and $u_{cj}(t)$ are the vertical displacement of the beam and displacement of the contact point, with $u_{cj}(t) = u(x,t)|_{x=v(t-t_j)}$, and $t_f = 0$ and $t_r = d/v$ the entry times of the front and rear axles.

In order to get a succinct analytical solution for the bridge and contact points, the bridge considered is a simply supported uniform Bernoulli-Euler beam of span length L, per-unit-length mass m, elastic modulus E, and moment of inertia I. The equation of equilibrium for the vertical motion of the beam under the moving vehicle is

$$m\ddot{u}(x,t) + EIu(x,t)'''' = F(t), \tag{4}$$

where the prime ($'$) denotes the spatial derivative. Assuming that the mass of the two-axle vehicle is much smaller than that of the bridge, i.e., $M_v + m_{wf} + m_{wr} \ll mL$, the inertial effect of the test vehicle on the bridge response can be neglected [65]. Therefore, the contact force $F(t)$ arising from the vehicle's front and rear axle loads p_j ($j = f, r$) can be represented as

$$F(t) = \sum_{j=f,r} p_j\delta\left[x - v\left(t - t_j\right)\right]\left[H\left(t - t_j\right) - H\left(t - t_j - T\right)\right], \tag{5}$$

where δ and H denote Dirac' delta and unit step functions, respectively, T the travel time ($= L/v$), and p_j the front and rear axle loads, i.e.,

$$p_j = \frac{\left[(d - d_j)M_v + m_{wj}\right]g}{d}, \qquad j = f, r \tag{6}$$

and g is the acceleration of gravity.

By modal superposition, the displacement of the beam can be obtained [10]

$$u(x,t)=\sum_{n=1}^{N}\sum_{j=f,r}\frac{\Delta_{stn,j}}{1-S_n^2}\begin{bmatrix}\sin\dfrac{n\pi v(t-t_j)}{L}\\ -S_n\sin\omega_{b,n}(t-t_j)\end{bmatrix}\begin{bmatrix}H(t-t_j)\\ -H(t-t_j-T)\end{bmatrix}\sin\frac{n\pi x}{L}, \quad (7)$$

where $\omega_{b,n}$ is the nth frequency of the beam, S_n the speed parameter, $\Delta_{nst,j}$ the nth modal static deflection caused by p_j,

$$\omega_{b,n}=\frac{n^2\pi^2}{L^2}\sqrt{\frac{EI}{m}},\qquad S_n=\frac{n\pi v}{L\omega_{b,n}},\qquad \Delta_{stn,j}=\frac{2p_jL^3}{n^4\pi^4EI} \quad (8a\text{-}c)$$

Letting $x=v(t-t_j)$ to represent the contact location of the jth axle on the bridge yields the contact displacement $u_{cj}(t)$ as

$$\begin{aligned}u_{cj}(t)=\sum_{n=1}^{N}\sum_{i=f,r}\frac{\Delta_{stn,i}}{1-S_n^2}\left[\sin\frac{n\pi v(t-t_i)}{L}-S_n\sin\omega_{b,n}(t-t_i)\right][H(t-t_i)\\ -H(t-t_i-T)]\sin\frac{n\pi v(t-t_j)}{L},\qquad j=f,r.\end{aligned} \quad (9)$$

Taking the second derivative of Eq. (9) yields the contact acceleration $\ddot{u}_{cj}(t)$, which is not shown here for brevity. The contact accelerations obtained in this section is referred to as the analytical solution and will be used as a reference in the subsequent numerical simulation analysis. Clearly, one finds form Eq. (9) that the frequencies of the two-axle vehicle have been excluded from the expression of the front and rear contact responses.

In reality, it is difficult to directly measure the accelerations of the contact points as they move along with the vehicle over the test bridge. Nevertheless, by using the equilibrium equations of the test vehicle, the contact accelerations $\ddot{u}_{cj}(t)$ can be back-calculated from the responses of the test vehicle and has been verified by field tests [3]. For the two-axle vehicle considered, the back-calculated formulas are given as follows

$$\ddot{u}_{cj}(t)=\frac{1}{c_{wj}}e^{\frac{-k_{wj}}{c_{wj}}t}\int_0^t F_{wj}(\tau)\,e^{\frac{k_{wj}}{c_{wj}}\tau}\mathrm{d}\tau,\qquad j=f,r, \quad (10)$$

where

$$\begin{aligned}F_{wj}(t)=m_{wj}\frac{\mathrm{d}^2\ddot{y}_{wj}}{\mathrm{d}t^2}+c_{wj}\frac{\mathrm{d}\ddot{y}_{wj}}{\mathrm{d}t}+k_{wj}\ddot{y}_{wj}+c_{sj}\left[\frac{\mathrm{d}\ddot{y}_{wj}}{\mathrm{d}t}-\frac{\mathrm{d}\ddot{y}_{vj}}{\mathrm{d}t}\right]\\ +k_{sf}\left[\ddot{y}_{wj}-\ddot{y}_{vj}\right].\end{aligned} \quad (11)$$

And $\ddot{y}_{wj}$ can be back-calculated from the vehicle's body responses, i.e.,

$$\ddot{y}_{wj}(t)=\frac{1}{c_{sj}}e^{\frac{-k_{sj}}{c_{sj}}t}\int_0^t F_{sj}(\tau)\,e^{\frac{k_{sj}}{c_{sj}}\tau}\mathrm{d}\tau,\qquad j=f,r, \quad (12)$$

where

$$F_{sf}(t)=\left(\frac{d_rM_v}{d}\right)\frac{\mathrm{d}^2\ddot{y}_v}{\mathrm{d}t^2}-\left(\frac{J_v}{d}\right)\frac{\mathrm{d}^2\ddot{\theta}_v}{\mathrm{d}t^2}+k_{sf}\left[\ddot{y}_v-d_f\ddot{\theta}_v\right]+c_{sf}\left[\frac{\mathrm{d}\ddot{y}_v}{\mathrm{d}t}-d_f\frac{\mathrm{d}\ddot{\theta}_v}{\mathrm{d}t}\right], \quad (13a)$$

$$F_{sr}(t)=\left(\frac{d_f M_v}{d}\right)\frac{\mathrm{d}^2\ddot{y}_v}{\mathrm{d}t^2}+\left(\frac{J_v}{d}\right)\frac{\mathrm{d}^2\ddot{\theta}_v}{\mathrm{d}t^2}+k_{sr}\left[\ddot{y}_v+d_r\ddot{\theta}_v\right]+c_{sr}\left[\frac{\mathrm{d}\ddot{y}_v}{\mathrm{d}t}+d_r\frac{\mathrm{d}\ddot{\theta}_v}{\mathrm{d}t}\right]. \quad (13b)$$

3 Recovery of Bridge Mode Shapes

To identify mode shapes of the bridge, the bridge component responses that are of concern can be singled out from the front and rear contact responses by techniques such as bandpass filter and mode decomposition techniques. For illustration, the case when the vehicle's two wheels are acting simultaneously on the bridge is considered. By assuming the driving frequency $n\pi v/L$ is much smaller than the bridge frequency $\omega_{b,n}$, the bridge acceleration component response can be obtained from the theoretical contact displacement in Eq. (9), i.e.,

$$\ddot{u}_{cj}(t)=\sum_{n=1}^{N}\frac{-S_n\omega_{b,n}^2}{1-S_n^2}\begin{bmatrix}\Delta_{stn,f}\sin\omega_{b,n}(t-t_f)\\+\Delta_{stn,r}\sin\omega_{b,n}(t-t_r)\end{bmatrix}\sin\frac{n\pi v(t-t_j)}{L}, j=f,r. \quad (14)$$

By using trigonometric function formulas, one can obtain the acceleration of the contact point $\ddot{u}_{cj,n}(t)$ as:

$$\ddot{u}_{cj}(t)=\sum_{n=1}^{N}\frac{S_n\omega_{b,n}^2K}{1-S_n^2}A_j(t)\cos(\omega_{b,n}t+\theta_0), \qquad j=f,r, \quad (15)$$

where

$$K=\sqrt{\Delta_{stn,f}^2+\Delta_{stn,r}^2+2\Delta_{stn,f}\Delta_{stn,r}\cos\omega_{b,n}(t_f-t_r)}, \quad (16a)$$

$$A_j(t)=\sin\frac{n\pi v(t-t_j)}{L}, \qquad j=f,r, \quad (16b)$$

$$\theta_0=\tan^{-1}\left(\frac{\Delta_{stn,f}\cos(\omega_{b,n}t_f)+\Delta_{stn,r}\cos(\omega_{b,n}t_r)}{\Delta_{stn,f}\sin(\omega_{b,n}t_f)+\Delta_{stn,r}\sin(\omega_{b,n}t_r)}\right). \quad (16c)$$

Subsequently, the WT of contact acceleration $\ddot{u}_{cj,n}(t)$ can be obtained,

$$W_{cj}(a,b)=\frac{\sqrt{a}}{2}\sum_{n=1}^{N}\frac{S_n\omega_{b,n}^2K}{1-S_n^2}A_j(b)\boldsymbol{\Psi}^*(a\omega_{b,n})e^{i(\omega_{b,n}b+\theta_0)}, \qquad j=f,r. \quad (17)$$

For a fixed value of the dilatation parameter a_n, $|W_{cj}(a,b)|$ reaches the maximum at $a_n=\omega_0/\omega_{b,n}$ for the nth bridge component response, i.e.,

$$|W_{cj,n}(a_n,b)|=\left|\frac{\sqrt{a_n}}{2}\frac{S_n\omega_{b,n}^2K}{1-S_n^2}A_j(b)\boldsymbol{\Psi}^*(a_n\omega_{b,n})\right|, \qquad j=f,r. \quad (18)$$

In this study, the wavelet coefficients of the front and rear contact points are used to identify mode shapes of the bridge. For a certain moment (i.e., time parameter b_k), letting the front contact point be the response point, and the rear contact point be the reference point, the ratio $\varphi_{f,r}$ of the wavelet coefficients for the front and rear contact point responses can be obtained, i.e.,

$$\varphi_{f,r}(a_n,b_k)=\left|\frac{W_{cf,n}(a_n,b_k)}{W_{cr,n}(a_n,b_k)}\right|=\left|\frac{\frac{\sqrt{a}}{2}\frac{S_n\omega_{b,n}^2K}{1-S_n^2}A_f(b_k)\boldsymbol{\Psi}^*(a_n\omega_{b,n})}{\frac{\sqrt{a}}{2}\frac{S_n\omega_{b,n}^2K}{1-S_n^2}A_r(b_k)\boldsymbol{\Psi}^*(a_n\omega_{b,n})}\right| \quad (19)$$

$$= \left|\frac{A_f(b_k)}{A_r(b_k)}\right| = \left|\frac{\sin\frac{n\pi v b_k}{L}}{\sin\frac{n\pi v(b_k - t_r)}{L}}\right|,$$

The ratio $\varphi_{f,r}$ of the wavelet coefficients will be updated for interval $\Delta b = t_r = d/v$ as the two-axle test vehicle (and contact points) moves forward. Therefore, the *n*th bridge mode shape can be obtained as

$$\Phi_k(a_n, b_k) = \Phi_{k-1}(a_n, b_{k-1})\varphi_{f,r}(a_n, b_k) \quad (20)$$

By assuming the wavelet coefficient of the initial reference point to be unity, i.e., $\Phi_0(a_n, b_0) = 1$, the amplitudes of the *n*th bridge mode shape can be calculated at each iteration step. However, the amplitude of the bridge mode shapes is given in absolute value. The final mode shapes should be adjusted based on engineer's judgment and experience.

4 Numerical Study

4.1 Verification of back-calculation procedure for contact responses

To illustrate the accuracy of the procedure for calculating contact responses, no other signal processing technique will be applied. For the two-axle test vehicle moving at $v = 5$ m/s (18 km/h) [10], the vehicle body's vertical and rotational acceleration spectra have been plotted in Figure 2(a) and (b), respectively. One finds from the spectra in Figure 2 that the 1st bridge frequency can be clearly identified, the amplitude of the 2ed bridge frequency drops rapidly, and the 3rd bridge frequency cannot be recognized in the vehicle body's vertical response (Figure 2(a)), but marginally visible in the vehicle body's rotational response (Figure 2(b)).

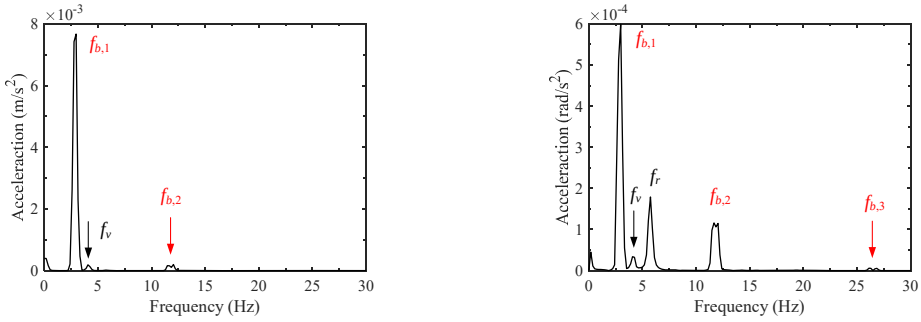

(a) (b)

Figure 2 Spectra of vehicle body's responses: (a) vertical; (b) rotational.

Based on the vehicle body's vertical and rotational responses (made available by FEM) and front and rear wheel responses (available by back-calculation formula in Eq. (12)), the front and rear contact responses can be back-calculated by Eq. (10), as shown in Figure 3. Evidently, one finds from Figure 3 that the contact responses calculated by the proposed back-calculation formula in Eq. (10) match very well with the analytical and FEM solutions for both front and rear responses, which is an indication that the procedure for calculating the contact responses using Eq. (10) is highly reliable. One can find from the spectra in Figure 3 that the vehicle frequencies have been eliminated from the front and rear contact responses. In addition, the first

three bridge frequencies appear quite outstanding in the contact response spectra. A comparison of the contact spectra in Figure 3 with the vehicle's body spectra in Figure 2 indicates that contact responses outperform the vehicle responses in that more bridge frequencies of high orders can be identified.

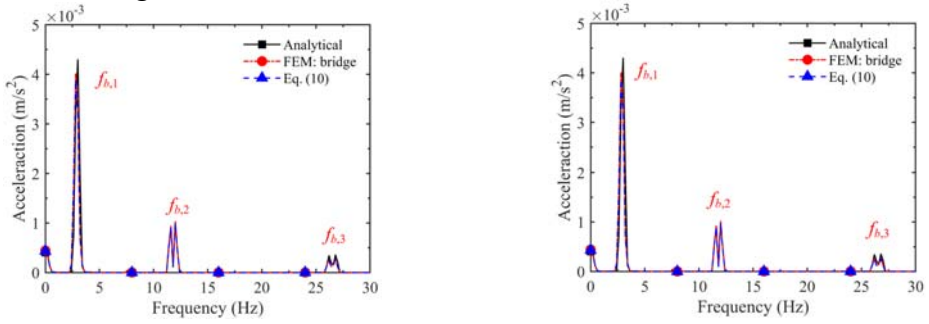

(a) (b)

Figure 3 Spectra of contact responses: (a) front contact point; (b) rear contact point.

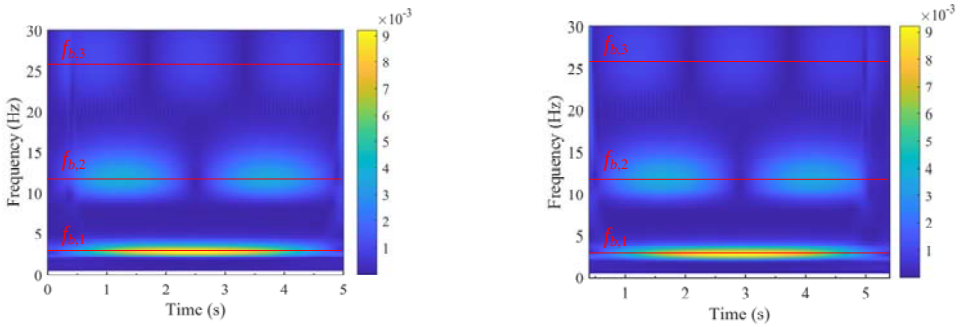

(a) (b)

Figure 4 WT results of: (a) front contact response; (b) rear contact response.

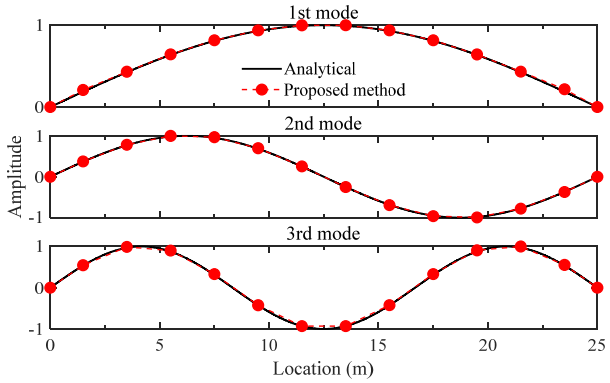

Figure 5 Bridge mode shapes recovered from the front contact response.

4.2 Recovery of bridge mode shapes by the WT

The reliability of the procedure for recovering mode shapes of the bridge using WT will be assessed in the following. The wavelet coefficients of the front and rear contact responses obtained by applying the WT have been plotted in Figure 4(a) and (b), respectively. As can be seen from Figure 4(a) and (b), the identified bridge frequencies

are marked with red lines on the time-frequency diagrams (i.e., $\left|W_{cj}(a_n, b)\right|$ reaches the maximum as the condition $a_n = f_0/f_{b,n}$ is met for each bridge component). Subsequently, applying the procedures for recovering bridge mode shapes, one can obtain the first three mode shapes of the bridge, which have been plotted in Figure 5. Obviously, one can find from Figure 5 that the first three mode shapes of the bridge recovered by the present procedure match well the theoretical ones. For the present case, the modal assurance criterion (MAC) values for the first three mode shapes in Figure 5 are 0.999, 0.999, and 0.999, which indicates that the mode shapes of the bridge identified by the present procedure are of high accuracy.

5 Conclusions

In this study, wavelet transform (WT) is theoretically investigated to extract bridge mode shapes from a passing two-axle test vehicle. Firstly, closed-form solutions for the dynamic responses of the bridge and front and rear contact points are derived. Secondly, to overcome the masking effect by vehicle's self frequencies on bridge frequencies in the vehicle's spectra, the procedure for calculating contact responses of a two-axle test vehicle considering the suspension effect was derived. Next, the WT is theoretically investigated to construct the bridge mode shapes via the use of the correlation between the front and rear contact points. The feasibility of the proposed method for constructing mode shapes was successfully verified by the numerical study.

Acknowledgements

This research reported herein is sponsored by the following agencies: National Natural Science Foundation of China (Grant No. 52208146 and 52078082), Chongqing Science and Technology Commission (Grant No. CSTB2022NSCQ-MSX1471 and 2022YSZX-JSX0004CSTB), and China Postdoctoral Science Foundation (Grant No. 2022M720580).

References

[1] Y.B. Yang, C.W. Lin, J.D. Yau. Extracting bridge frequencies from the dynamic response of a passing vehicle, *J. Sound Vib.* 2004, 272: 471-493.

[2] S. Urushadze, J.D. Yau. Experimental verification of indirect bridge frequency measurement using a passing vehicle, *Procedia Eng.* 2017, 190: 554–559.

[3] Y.B. Yang, H. Xu, B. Zhang, F. Xiong, Z.L. Wang. Measuring bridge frequencies by a test vehicle in non-moving and moving states, *Eng. Struct.* 2020, 203: 109859.

[4] Z.L. Wang, J.P. Yang, K. Shi, H. Xu, F.Q. Qiu, Y.B. Yang. "Recent advances in researches on vehicle scanning method for bridges," *Int. J. Struct. Stab. Dyn.* 2022, DOI: 10.1142/S0219455422300051.

[5] Y.B. Yang, Y.C. Li, K.C. Chang. Constructing the mode shapes of a bridge from a passing vehicle: A theoretical study, *Smart Struct. Syst.* 2014, 13(5): 797–819.

[6] A. Malekjafarian, E.J. OBrien. Identification of bridge mode shapes using short time frequency domain decomposition of the responses measured in a passing vehicle, *Eng. Struct.* 2017, 81: 386-397.

[7] X. Kong, C.S. Cai, L. Deng, W. Zhang. Using dynamic responses of moving vehicles to extract bridge modal properties of a field bridge, *J. Bridge Eng.* 2017, 22(6): 04017018.
[8] S.S. Eshkevari, S.N. Pakzad, M. Takác, T.J. Matarazzo. Modal identification of bridges using mobile sensors with sparse vibration data, *J. Eng. Mech.* 2020, 146(4): 04020011.
[9] X. Jian, Y. Xia, L. Sun. An indirect method for bridge mode shapes identification based on wavelet analysis, *Struct. Control Health Monit.* 2020, 27(12): e2630.
[10] H. Xu, Y.H. Liu, M. Yang, D.S. Yang, Y.B. Yang. Mode shape construction for bridges from contact responses of a two-axle test vehicle by wavelet transform, *Mech. Syst. Signal Process.*, 2023, 195: 110304